

Article

The Statistical Characteristics Analysis for Overvoltage of Elevated Transmission Line under High-Altitude Electromagnetic Pulse Based on Rosenblatt Transformation and Polynomial Chaos Expansion

Zheng Liu ^{*,†} , Dongwei Hei, Congguang Mao, Chuanbao Du, Xin Nie, Wei Wu and Wei Chen

State Key Laboratory of Intense Pulsed Radiation Simulation and Effect, Northwest Institute of Nuclear Technology, Xi'an 710024, China

* Correspondence: xjtlz94@163.com

† Zheng Liu received his bachelor degree at the department of Electronics Science and Technology of Xi'an Jiaotong University in 2016 and Master Degree at the Department of Nuclear Technology and Engineering from Northwest Institute of Nuclear Technology. Now he is a researcher of State Key Laboratory of Intense Pulsed Radiation Simulation and Effect of Northwest Institute of Nuclear Technology, which mainly focus on the EMP environment calculation and experiment.

Abstract: A High-Altitude Electromagnetic Pulse (HEMP) could induce very fast transient overvoltage (VFTO) with nanosecond level rise time and mega-volt amplitude, which severely threatens the electrical devices connected to the elevated transmission line. An elevated transmission line with different locations may suffer different levels of HEMP threat since the dip angle could influence the polarization of the HEMP wave. The combination of Rosenblatt Transformation and Polynomial Chaos Expansion (R-PCE) is introduced in this paper. With this method, the efficiency of calculating the overvoltage of an elevated transmission line under HEMP is improved, speeding up 24.75 times. The influence of different factors (dip angle, elevated height, and earth conductivity) on the overvoltage of elevated transmission lines applied in power systems is calculated and analyzed. The numerical result shows with 99.9% confidence that the overvoltage would be over 3.7 MV of amplitude and 6.7×10^{14} V/s of voltage derivative, which is much more rigorous than a lightning pulse. We also find that elevated transmission lines may have a larger HEMP threat in a small dip angle area. The corresponding data are shown at the end of the paper, which could be useful for relative researchers in pulse injection experiments and reliable evaluation.

Keywords: High-Altitude Electromagnetic Pulse (HEMP); VFTO; transmission line; Rosenblatt Transformation; Polynomial Chaos Expansion; Monte Carlo; dip angle



Citation: Liu, Z.; Hei, D.; Mao, C.; Du, C.; Nie, X.; Wu, W.; Chen, W. The Statistical Characteristics Analysis for Overvoltage of Elevated Transmission Line under High-Altitude Electromagnetic Pulse Based on Rosenblatt Transformation and Polynomial Chaos Expansion. *Energies* **2023**, *16*, 4622. <https://doi.org/10.3390/en16124622>

Academic Editor: Federico Barrero

Received: 6 April 2023

Revised: 5 June 2023

Accepted: 6 June 2023

Published: 10 June 2023



Copyright: © 2023 by the authors. Licensee MDPI, Basel, Switzerland. This article is an open access article distributed under the terms and conditions of the Creative Commons Attribution (CC BY) license (<https://creativecommons.org/licenses/by/4.0/>).

1. Introduction

The electrical grid has become more complicated and vulnerable to unusual electromagnetic phenomena, such as very fast transient overvoltage (VFTO), due to more electronics and informational devices being used. High-Altitude Electromagnetic Pulse (HEMP) could induce a fast, high-amplitude current or voltage pulse on the transmission line, threatening the devices connected to the transmission line, such as metal oxide arresters, insulators, and transformers [1–6]. Because the whole electrical grid cannot be tested under a HEMP radiation wave simulator, such as a vertical or horizontal polarization device, the main testing method is to use pulse injection, which injects the energy of a HEMP into the electrical equipment. The energy of pulse injection is expressed by short current or open voltage, and the value of this energy is calculated using the statistical characteristics of the response of the transmission line under a HEMP [7,8]. However, the statistical characteristics for the overvoltage of a transmission line under a HEMP could

vary dramatically with different parameter settings, such as elevated height, ground conductivity, and, especially, dip angle related to the line location. The usual way of obtaining the overvoltage is by solving a first-order ordinary differential equation, which has low efficiency in a traditional statistical calculation, for example, using the Monte Carlo Method despite its high robustness [9,10].

Recently, more and more researchers have pursued more efficient uncertainty calculation methods. Polynomial Chaos, expressing the response with orthogonal polynomials, can be regarded as a rational choice that transfers the uncertainty of response on the coefficients of the polynomial. It has been widely and sophisticatedly used in multiport systems, structural mechanics, and acoustic wave propagation [11–18]. As for the aspect of electromagnetic, the stochastic simulation of interconnects illuminated by random external fields is calculated based on Polynomial Chaos, and the uniform distribution is assumed. However, in a real situation, the distribution of variables in the propagation of a HEMP is not uniform when the randomness of the relationship between a HEMP burst and an elevated transmission line is considered. Moreover, there are several independent variables in the calculation of a HEMP response, and all uncertain variables for Polynomial Chaos are required to be independent. For this issue, the Rosenblatt transformation, as a type of probability integral transform, is available for approaching all kinds of distributions in a unified manner. At this time, all variables are independent of each other [19,20].

This paper establishes an efficient calculation method based on Rosenblatt transformation and Polynomial Chaos Expansion (R-PCE) to obtain the statistical characteristics for the open voltage response of an elevated transmission line. The variables and environmental parameters in calculating the HEMP response are listed and transformed into unified distribution using Rosenblatt transformation; hence, the method is available to Polynomial Chaos. Monte Carlo Samples verify the accuracy and efficiency of this method. According to the calculation results, we analyze the voltage peak and derivative of transmission line response under the influence of different ground conductivity, elevated height, and dip angle with a confidence of 99.9%. A comprehensive data table consisting of different heights and dip angles is shown, which could contribute to the pulse injection experiment and its reliable evaluation.

The rest of this article is organized as follows. Section 2 introduces the variables in HEMP propagation and efficient calculation methods combined with Rosenblatt transformation and Polynomial Chaos. In Section 3, the method is verified, and numerical results are analyzed. Finally, Section 4 concludes this article.

2. Variables Analysis and Calculation Methods

2.1. The Coupling Model of Transmission Line

Many researchers have studied the coupling model of elevated line and electromagnetic pulse, and Figure 1 shows a coupling model. The first way to calculate the response of an elevated line under a HEMP is by solving the telegraph equation in the frequency domain and transforming the results into the time domain with inverse fast Fourier transformation (IFFT), known as the transmission line (TL) method. It is easy to consider a lossy ground environment around the transmission line and could be solved by analytic expressions. However, the TL method might be questionable when the cross-section of the line is not small with respect to the wavelength at high frequencies under a quasi-transverse electromagnetic assumption. Meanwhile, there is radiation loss on the line due to the discontinuities at the line termination. The other methods are full wave techniques such as finite difference time domain (FDTD) or method of moments (MoM). The advantage of these methods is that they are highly accurate by solving the response step by step in the time domain. However, it is time-consuming and unacceptable to pursue a statistical calculation since the single-time cost of the full wave technique is hour-level for long elevated lines in the power system. Commonly, for the statistical calculation of the response of transmission lines under an electromagnetic pulse, the TL method is used.

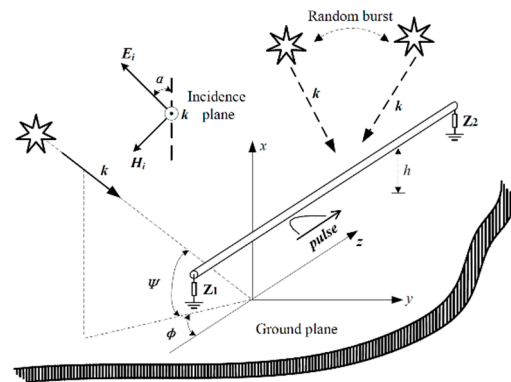


Figure 1. Random HEMP coupling to an elevated transmission line.

Because the TL model is a suitable alternative for the statistical calculation of long elevated transmission lines, much work to improve the model with the consideration of high-frequency correction has been pursued. For a conventional TL model in Figure 1, k , E_i , H_i and h are wave vector of HEMP, electric field intensity and magnetic field intensity, the height of the line, respectively. The voltage at terminals of the transmission line on a lossy ground is calculated by solving the Baum-Liu-Tesche (BLT) equation according to the following expression.

$$\begin{bmatrix} V(0) \\ V(L) \end{bmatrix} = \begin{bmatrix} 1 + \rho_1 & 0 \\ 0 & 1 + \rho_2 \end{bmatrix} \begin{bmatrix} -\rho_1 & e^{\gamma L} \\ e^{\gamma L} & -\rho_2 \end{bmatrix}^{-1} \begin{bmatrix} S_1 \\ S_2 \end{bmatrix} \quad (1)$$

where ρ_i is the voltage reflection coefficients at the line terminals, γ is the complex propagation constant of the transmission line, and S_i is the distributed voltage sources calculated from the incident electric field along the line path.

$$\rho_i = \frac{Z_i - Z_C}{Z_i + Z_C} \quad (2)$$

$$\gamma = \sqrt{Z'Y'} \quad (3)$$

$$\begin{bmatrix} S_1 \\ S_2 \end{bmatrix} = \begin{bmatrix} \frac{1}{2} \int_0^L e^{\gamma x} V'_{S2}(x) dx - \frac{V_1}{2} + \frac{V_2}{2} e^{\gamma L} \\ -\frac{1}{2} \int_0^L e^{(L-\gamma x)} V'_{S2}(x) dx + \frac{V_1}{2} e^{\gamma L} - \frac{V_2}{2} \end{bmatrix} \quad (4)$$

Z_C is the characteristic impedance of the transmission line. Z' and Y' are impedance and admittance of per-unit-length line, respectively. V'_{S2} is the sum of incident electric field and reflection electric field along the transmission line. R_v and R_h are the vertical and horizontal Fresnel reflection coefficients of a lossy ground.

$$\begin{aligned} V'_{S2} &= E_x^e \\ &= E_x^{inc} + E_x^{ref} \\ &= E_0 \left[\begin{array}{l} \cos \alpha \sin \psi \cos \phi \left(e^{jkz \sin \psi} - R_v e^{-jkz \sin \psi} \right) \\ + \sin \alpha \sin \phi \left(e^{jkz \sin \psi} + R_h e^{-jkz \sin \psi} \right) \end{array} \right] e^{-jkx \cos \psi \cos \phi} \end{aligned} \quad (5)$$

$$R_v = \frac{\epsilon_r [1 + \sigma_g / (j\omega\epsilon_r\epsilon_0)] \sin \psi - \{ \epsilon_r [1 + \sigma_g / (j\omega\epsilon_r\epsilon_0)] - \cos^2 \psi \}^{1/2}}{\epsilon_r [1 + \sigma_g / (j\omega\epsilon_r\epsilon_0)] \sin \psi + \{ \epsilon_r [1 + \sigma_g / (j\omega\epsilon_r\epsilon_0)] - \cos^2 \psi \}^{1/2}} \quad (6)$$

$$R_h = \frac{\sin \psi - \{ \epsilon_r [1 + \sigma_g / (j\omega\epsilon_r\epsilon_0)] - \cos^2 \psi \}^{1/2}}{\sin \psi + \{ \epsilon_r [1 + \sigma_g / (j\omega\epsilon_r\epsilon_0)] - \cos^2 \psi \}^{1/2}} \quad (7)$$

The voltage sources V_i at the terminations in this paper are calculated as the integral of the vertical field along the risers, as shown in Figure 2, and the increase in the effective line length because the vertical riser is not considered in this paper [21].

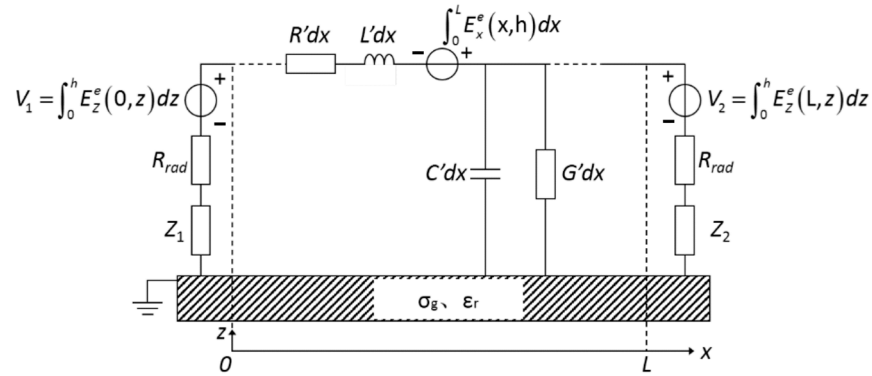


Figure 2. Modeling of transmission line with field variation and radiation resistances.

Meanwhile, additional resistance is introduced as the resistance of a radiating monopole to make a high-frequency correction in BLT equations and is considered in the voltage reflection coefficients [21].

$$R_{rad} = 160\pi^2 \left(\frac{h}{\lambda}\right)^2 \tag{8}$$

$$\rho_i = \frac{Z_i + R_{rad} - Z_C}{Z_i + R_{rad} + Z_C} \tag{9}$$

λ is the electromagnetic wavelength of a certain frequency. This radiating resistance is negligible at low frequencies and increases as a function of the frequency. Because the spectrum of the HEMP is so high, the losses increase dramatically for the transmission line response calculation. The radiating resistances are set at both ends of the transmission line. However, resistance only plays an important role when the termination value is comparable with radiating resistance. In this paper, the value of termination is 1 MΩ, which expresses the status of open voltage and the influence of different values of terminations on the voltage, as shown in Figure 3. In the calculation, the standard E1 HEMP waveform with 50 kV/m amplitude, 2.5 ns rise time, and 23 ns pulse width defined by IEC is selected.

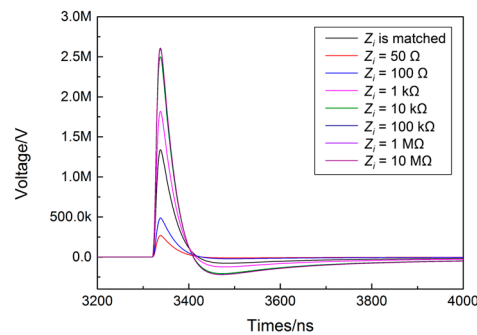


Figure 3. The influence of termination value on voltage (length = 1 km, height = 10 m, radius = 0.01 m, $\Psi = 5^\circ$, $\Phi = 0^\circ$, and $\alpha = 0^\circ$).

The characteristics of lossy ground are expressed as ground resistance depending on the relative permittivity of ground ϵ_r and ground conductivity δ_g :

$$Z'_g = \frac{j\omega\mu_0}{2\pi} \ln \frac{1 + \gamma_g h}{\gamma_g} \tag{10}$$

$$\gamma_g = \sqrt{j\omega\mu_0(\delta_g + j\omega\epsilon_r\epsilon_0)} \tag{11}$$

Z_g' approximates Sunde's formula for the per-unit length Earth return impedance, γ_g is the propagation constant of the electromagnetic wave in the ground, and h is the height of the elevated transmission line. Obviously, the ground parameters are frequency dependent in real situations and influenced by many factors, such as percentage moisture content. However, only a slight difference of less than 4% of coupling response is obtained according to the reference [21]. Therefore, in this paper, relative permittivity and ground conductivity are considered constant.

2.2. Variables in the HEMP Calculation

The random relationship between a HEMP burst and an elevated transmission line area (see Figure 4) causes uncertainty of the voltage response on the line. Different relationships between burst and transmission lines would cause the response to be different; therefore, the worst peak amplitude and derivative of voltage pulse would not exist in the same field-to-line situation. In conclusion, all the situations of the HEMP pulse incidence should be considered in the statistical calculation.

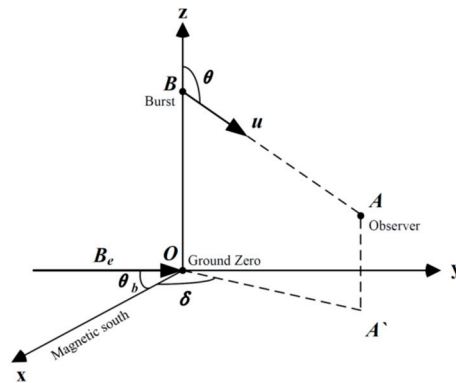


Figure 4. The relationship between HEMP burst (point B) and elevated transmission line (point A).

The relationship is shown in Figure 4; for an elevated transmission line A with a stationary location whose dip angle is not changed, the burst, B, is randomly distributed around elevated transmission line A.

In order to describe the randomness of HEMP propagation, there are four variables in the propagation of a HEMP pulse as follows.

2.2.1. Height of Burst, HOB

The HOB defines the vertical height between nuclear burst and earth ground. It is normally considered a unified distribution with a range of 50 to 400 km.

2.2.2. Elevation Angle Psi

As shown in Figure 1, the elevation angle is not only a non-classic distribution but also dependent; therefore, HOB could influence its type of distribution. The specific expression of the probability distribution function is shown below, where R defines the radius of Earth with the value of 6400 km [10].

$$F(\psi) = \left[1 + \frac{R}{HOB}\right] \sin \left[\Psi + \sin^{-1} \frac{\cos \psi}{1 + \frac{HOB}{R}} \right] - \frac{R}{HOB} \tag{12}$$

2.2.3. Orientation Angle δ

The definition of orientation angle is shown in Figure 4; since the relationship between the burst and the elevated transmission line is randomly distributed, it has a uniform distribution with the range from 0 to 2π .

2.2.4. Azimuthal Angle Φ

The definition of azimuthal angle Φ is shown in Figure 1; since the relationship between the burst and the elevated transmission line is randomly distributed and the elevated transmission line in the calculation is always considered as central symmetry, it has a type of uniform distribution with a range from 0 to $\pi/2$.

2.3. How Variables Influence HEMP Propagation

The vector u in Figure 4 defines the HEMP pulse from burst to the elevated transmission line, and Be defines Earth's magnetic field vector. The dip angle θ_{dip} between the magnetic south and the dip angle θ_{dip} would influence the polarization angle α of the HEMP pulse as follows.

$$\alpha = \arctan \left| \frac{\sin \theta \sin \theta_b - \cos \theta \cos \delta \cos \theta_b}{-\sin \delta \cos \theta_b} \right| \quad (13)$$

The line of sight angle θ shown in Figure 4 can be expressed as follows.

$$\theta = \pi - \arcsin \left(\frac{R}{R + HOB} \cos \psi \right) \quad (14)$$

As discussed above, the variables discussed in Section 2.2 are connected with the polarization angle α and the line of sight angle θ , which would influence the response of the elevated transmission line under a HEMP.

2.4. Norm for Coupling Response

There are two norms in the coupling process between the HEMP pulse and the elevated transmission line: peak value and max derivative. The peak value of voltage V_P is the infinite norm and denotes the max absolute value of open voltage in the time domain, which is connected with the level of HEMP threat.

$$V_P = |V(t)|_{\max} \quad (15)$$

The max derivative k_{\max} is also an infinite norm and denotes the max voltage derivative in the time domain. It reflects how fast the voltage changes during the pulse's rise time.

$$k_{\max} = \left| \frac{dV(t)}{dt} \right|_{\max} \quad (16)$$

As discussed above, the worst of these norm parameters would not occur in the same coupling situation. We need to obtain the statistical calculation so that specific norm parameters with certain confidence would be available for pulse injection experiments and relatively reliable evaluation of the electrical grid.

2.5. Efficient Calculation Method

In order to analyze the statistical characteristics of the voltage of elevated transmission lines under a HEMP with different parameter settings such as dip angle, elevated height, and ground conductivity, an efficient calculation method compared with the Monte Carlo method is necessary. Polynomial Chaos can transfer the uncertainty of random processes into coefficients, meaning the bulk cost is solving polynomial coefficients instead of sampling generation. To meet the requirement of Polynomial Chaos that all the variables

should be dependent, the Rosenblatt transformation is introduced here to decouple the dependence of variables.

2.5.1. Polynomial Chaos Expansion

The main reason for adopting Polynomial Chaos Expansion (PCE) is that it provides a compact closed form that is accurate in a statistical sense, and a non-intrusive PCE is used in this paper. The method of non-intrusive PCE relies only on a collection of response samples of the calculation model for the determination of PCE coefficients and is similar to the Monte Carlo method, yet it exploits specific assumptions to improve the accuracy and efficiency of the calculation. Actually, non-intrusive PCE is a kind of surrogate modeling, with fewer times of model calculations, coefficients, and basic functions constructing the surrogate model. The surrogate model could dramatically reduce the time cost of sample generation.

The voltage V_{OV} at the termination of the elevated transmission line under a HEMP could be regarded as a function of the variables $\xi = (HOB, \Psi, \delta, \Phi)^T$ in Section 2.2, which could be expanded by orthogonal polynomial L_i as follows.

$$\begin{aligned}
 V_{OV} = & a_0 L_0 \\
 & + \sum_{i=1}^n a_i L_1(\xi_i) \\
 & + \sum_{i=1}^n \sum_{j=1}^i a_{ij} L_2(\xi_i, \xi_j) \\
 & + \sum_{i=1}^n \sum_{j=1}^i \sum_{k=1}^j a_{ijk} L_3(\xi_i, \xi_j, \xi_k) \\
 & + \dots
 \end{aligned} \tag{17}$$

The expansion above can be truncated with the number of $m + 1$, which is related to the highest order of polynomial p and the number n of variables; n is 4 in this case.

$$V_{OV} = \sum_{i=0}^{m-1} c_i \varphi_i(\xi), m + 1 = \frac{(n + p)!}{n!p!} \tag{18}$$

According to the orthogonality of polynomials, the coefficients can be solved by calculating the inner product.

$$a_i = \langle V_{OV}(\xi), \varphi_i(\xi) \rangle / \langle \varphi_i(\xi)^2 \rangle \tag{19}$$

The statistical characteristics parameters, such as mean value μ and variance σ^2 are available as follows.

$$\mu = a_0, \quad \sigma^2 = \sum_{i=1}^{m-1} [a_i^2 \langle \varphi_i^2 \rangle] \tag{20}$$

2.5.2. Rosenblatt Transformation

It is important that the elevation angle Ψ here is a dependent variable which means the Polynomial Chaos expressed above cannot be used directly now, according to Formula (4), that the elevation angle Ψ is relative to HOB .

Rosenblatt transformation offers a way that, given the actual conditional distribution, we can transform the variable to independent and identically distributed uniform random variables. For a non-uniform distributed variables vector $\xi = (\xi_1, \xi_2, \dots, \xi_n)^T$, according

to the principle of equal probability changing, ξ can be transformed into a variable vector $\eta = (\eta_1, \eta_2, \dots, \eta_n)^T$ with uniform distribution of range from 0 to 1 as follows [21].

$$\begin{aligned} F_{\eta_1}(\eta_1) &= F_{\xi_1}(\xi_1) \\ F_{\eta_2}(\eta_2|\eta_1) &= F_{\xi_2}(\xi_2|\xi_1) \\ &\vdots \\ F_{\eta_n}(\eta_n|\eta_1, \eta_2, \dots, \eta_{n-1}) &= F_{\xi_n}(\xi_n|\xi_1, \xi_2, \dots, \xi_{n-1}) \end{aligned} \tag{21}$$

Then the specific dependent variables are transformed into independent ones by solving the equation below.

$$\begin{cases} \eta_1 = F_{\eta_1}^{-1}(F_{\xi_1}(\xi_1)) \\ \eta_2 = F_{\eta_2}^{-1}(F_{\xi_2}(\xi_2|\xi_1)|\eta_1) \\ \vdots \\ \eta_n = F_{\eta_n}^{-1}(F_{\xi_n}(\xi_n|\xi_1, \xi_2, \dots, \xi_{n-1})|\eta_1, \eta_2, \dots, \eta_{n-1}) \end{cases} \tag{22}$$

As for the elevation angle Ψ depending on the HOB , it can be expressed by a variable η_1 with a type of uniform distribution with the range from 0 to 1. The Newton-iteration method is used to solve the equation below.

$$\begin{cases} F_{\eta_1}(\eta_1) = F_{HOB}(HOB) \\ F_{\eta_2}(\eta_2|\eta_1) = \left[1 + \frac{R}{HOB}\right] \sin \left[\Psi + \sin^{-1} \frac{\cos \psi}{1 + \frac{HOB}{R}} \right] - \frac{R}{HOB} \end{cases} \tag{23}$$

3. Method Verification and Numerical Results

Regarding Rosenblatt transformation, all the variables discussed in Section 2.2 are decoupled and can be used in Polynomial Chaos to calculate the statistical characteristics for the response of an elevated transmission line under a HEMP pulse. Here, we assumed that HOB has a type of uniform distribution with a range from 50 to 400 km. The cumulative distribution probability of elevation angle Ψ calculated by the Monte Carlo method and Rosenblatt transformation is shown in Figure 5, which means the two methods fit well.

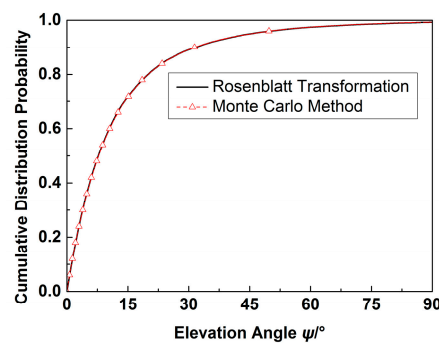


Figure 5. The cumulative distribution probability of elevation angle Ψ using Monte Carlo and Rosenblatt Transformation.

Then, we assumed an elevated transmission line with a length of 2000 m, a height of 10 m, a line radius of 0.01 m, and terminated by a high resistance of 1 M Ω at both sides of the line. The relative permittivity constant is 10 and 0.01 for the ground conductivity. Meanwhile, the incidence waveform of the HEMP here is from [22], which is a double exponential wave with an amplitude of 50 kV/m, a rise time of 2.5 ns, and a pulse width of 23 ns.

In this verification, we generate 246,240 Monte Carlo samples which are required by IEC 61000-2-10 and its reference [10]. Meanwhile, 10 Gauss integral points are used to calculate 7-order Polynomial Chaos Expansion. Because all the variables after the

Rosenblatt transformation have the type of uniform distribution, the Legendre polynomial is introduced in the Polynomial Chaos Expansion. The mean value and standard deviation of the open voltage of an elevated transmission line under a HEMP using the Polynomial Chaos and Monte Carlo method are shown in Figure 6. It is obvious that the two methods fit well. According to Equation (13), well-fitting of mean values, means, and standard deviation indicates that the integral accuracy and the order of Polynomial Chaos Expansion are acceptable, respectively. In the same computing situation, the time costs are 0.53 h and 13.12 h for Polynomial Chaos Expansion and Monte Carlo, respectively, which means Polynomial Chaos has 24.75 times efficiency improvement.

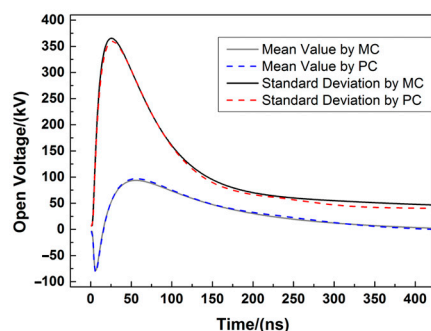


Figure 6. The verification of Polynomial Chaos Expansion compared with the Monte Carlo method.

With the higher efficiency of Polynomial Chaos Expansion, we can calculate different parameters' influence on the overvoltage response of elevated transmission lines under a HEMP with 99.9% confidence. First, voltage peak value and max derivative with different elevated heights and ground conductivity are calculated, as shown in Figure 7.

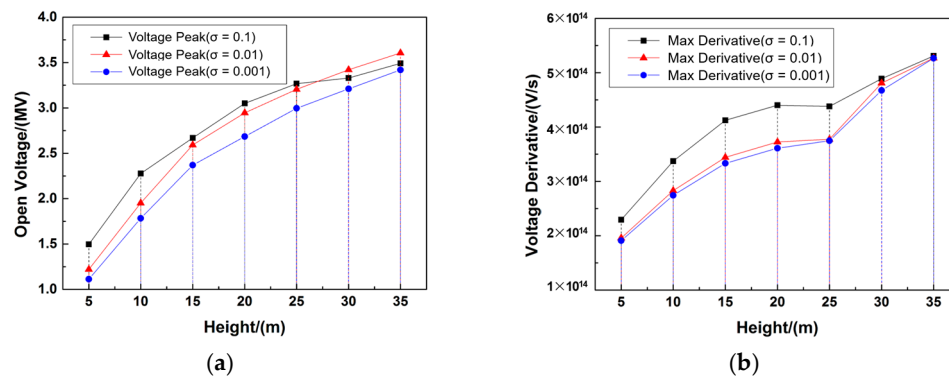


Figure 7. Different norms of overvoltage with different elevated transmission line heights and ground conductivity: (a) Voltage peak value; (b) Voltage max derivative.

The electrical grid has a large-range distribution, and the dip angle is relative to the polarization of the HEMP wave; hence, elevated transmission lines in different locations would suffer different levels of HEMP threat. In order to analyze this difference, using the results in Figure 7, we set the value of 0.1 for the ground conductivity to determine how the dip angle influences the voltage of the elevated transmission line with 99.9% confidence.

Corresponding calculation results are shown in Figure 8. It is clear that with the increasing dip angle, the norm of overvoltage response, such as voltage peak value and max derivative, all decrease in most situations. This means that in the area with a small dip angle and also a low-latitude area, the elevated transmission line may face a more rigorous HEMP environment, with higher overvoltage and faster voltage derivative. Especially for the norm of voltage derivative, nowadays, normal electromagnetic pulse protections on elevated transmission lines are prepared for lighting pulses; however, the max voltage derivative for lines over the height of 5 m from calculation results are all over 1.0×10^{14} V/s

and the max value is 6.7×10^{14} V/s which is far more than 1.0×10^{12} V/s for the direct effect of lighting environment according to MIL-STD-464. The max open voltage peak is over 3.7 MV, which might hardly damage the devices terminating the elevated transmission line. The most probable phenomenon is insulator surface flashover and overvoltage of metal oxide arresters and transformer. The primary effect of a HEMP on the elevated transmission line is from its speedy rise time and high amplitude. With the high efficiency of Polynomial Chaos, plenty of voltage peak and derivative data are available to us, and some of them, with a certain confidence, are listed in Tables 1 and 2. With these data, we can set the value of pulse voltage injection on the electrical devices, which terminates the transmission line according to the actual parameters such as line height and the location of the line. Meanwhile, the results of pulse voltage injection could also certify whether the electrical devices are able to resist the energy of a HEMP or which level of confidence the devices are able to resist. Furthermore, the damage data from pulse injection would be introduced into the vulnerability model of assessment to calculate the failure of the whole system caused by the HEMP interfaces.

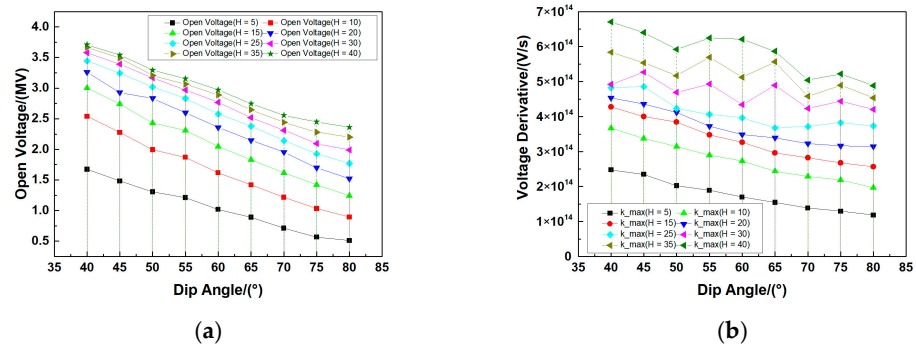


Figure 8. Different norms of overvoltage with different elevated transmission line heights and dip angle: (a) Voltage peak value; (b) Voltage max derivative.

Table 1. Different confidence levels for voltage peak for elevated transmission line (Values are in MV).

Height	10 m			20 m			30 m			40 m			
	Confidence	50%	90%	99%	50%	90%	99%	50%	90%	99%	50%	90%	99%
Dip Angle/°													
40		0.26	0.62	1.58	0.47	0.97	1.97	0.68	1.25	2.25	0.87	1.47	2.44
45		0.24	0.61	1.39	0.44	0.97	1.85	0.62	1.23	2.15	0.79	1.45	2.36
50		0.23	0.61	1.28	0.40	0.97	1.77	0.57	1.22	2.05	0.73	1.43	2.31
55		0.21	0.61	1.17	0.37	0.97	1.65	0.53	1.22	2.02	0.66	1.43	2.28
60		0.20	0.60	1.04	0.36	0.96	1.59	0.48	1.20	1.95	0.60	1.40	2.22
65		0.20	0.60	0.95	0.34	0.95	1.49	0.46	1.21	1.90	0.56	1.42	2.19
70		0.19	0.59	0.87	0.33	0.95	1.43	0.44	1.21	1.83	0.53	1.42	2.13
75		0.19	0.59	0.82	0.33	0.95	1.37	0.43	1.22	1.79	0.50	1.42	2.10
80		0.19	0.58	0.79	0.32	0.95	1.34	0.42	1.21	1.75	0.49	1.41	2.06

Table 2. Different confidence levels for voltage derivative for elevated transmission line (Values are in 10^{14} V/s).

Height	10 m			20 m			30 m			40 m			
	Confidence	50%	90%	99%	50%	90%	99%	50%	90%	99%	50%	90%	99%
Dip Angle/°													
40	0.69	1.26	2.08	1.05	2.02	2.80	1.22	2.67	3.71	1.30	3.30	4.56	
45	0.63	1.18	1.95	0.97	1.86	2.71	1.13	2.43	3.54	1.20	3.00	4.31	
50	0.57	1.12	1.85	0.87	1.73	2.58	1.02	2.21	3.34	1.09	2.71	4.00	
55	0.52	1.07	1.73	0.79	1.57	2.47	0.92	2.00	3.17	0.98	2.41	3.69	
60	0.46	1.00	1.66	0.71	1.44	2.40	0.82	1.78	2.95	0.89	2.12	3.42	
65	0.42	0.97	1.60	0.62	1.30	2.29	0.74	1.59	2.86	0.79	1.86	3.27	
70	0.38	0.93	1.53	0.55	1.20	2.22	0.64	1.41	2.70	0.70	1.61	3.05	
75	0.34	0.90	1.50	0.47	1.12	2.18	0.55	1.26	2.61	0.60	1.38	2.91	
80	0.32	0.87	1.48	0.40	1.07	2.10	0.45	1.16	2.52	0.49	1.20	2.78	

4. Discussion

Using the Rosenblatt transformation and Polynomial Chaos Expansion, the statistical calculation for open voltage of elevated transmission lines under a HEMP is sped up almost 25 times. With its high efficiency, multifold HEMP coupling situations with different parameters are listed, which indicates how these parameters influence the elevated transmission line's response. All the statistical calculations are modeled on the basis of typical HEMP environment variables proposed by W. A. Radasky, which were cited in the IEC 61000-2-10 standard to calculate a HEMP conducted environment [7,10]. However, with the development of research on power systems' effect under a HEMP, the characteristics of voltage gains more and more attention. According to the calculation results, a higher ground conductivity could cause the overvoltage to be larger than others, which is different from the short current. As for a large-range distribution of the electrical grid, the overvoltage of elevated transmission lines in different areas with 99% confidence is shown, and we found that lines in low-latitude areas may suffer a more rigorous HEMP threat by not only overvoltage peak but also voltage derivative.

According to the published record data, a 110 kV power transmission line has a max voltage value of 5.0 MV and 10 kV/m max voltage derivative by lightning pulse. Among all the calculation data, the max voltage is over 3.7 MV, and the max voltage derivative is over 6.7×10^{14} V/s, indicating that the derivative induced by a HEMP is almost 67 times harder than lightning with the nearly same voltage. Therefore, the devices applied in the electrical grid, especially in low-latitude areas, need more consideration to prevent damage from a HEMP.

Meanwhile, it is necessary to note that all the calculations here are based on the analysis of open voltage without considering the effect of the devices terminating the elevated transmission line, though much coupling data have been shown in this work. The main reason we use the open voltage is that the operational status of protection devices is typically open and connected to terminations. However, the nonlinear phenomena are essential when protecting devices that suffer the VFTO. We would model devices such as metal oxide arresters, insulators, or transformers directly connected to the elevated transmission line and then calculate their statistical characteristics under a HEMP in future research.

Author Contributions: Z.L., D.H., and C.M. conceived the presented idea; Z.L. and C.D. conducted the investigation; Z.L. and C.D. prepared the numerical integral program and calculated all the data; Z.L., C.M. and X.N. analyzed the numerical results; Z.L. primarily wrote the manuscript; C.M., W.W.,

and W.C. reviewed and edited the manuscript. All authors have read and agreed to the published version of the manuscript.

Funding: This research was funded by the State Key Laboratory of Intense Pulsed Radiation Simulation and Effect Foundation, grant number SKLIPR1904Z.

Data Availability Statement: Not applicable.

Conflicts of Interest: The authors declare no conflict of interest.

References

1. Mao, C.; Cheng, Y.; Xie, Y. *High Altitude Electromagnetic Pulse Technology Foundation*; Science Press: Beijing, China, 2019. (In Chinese)
2. Lyu, Y.; Wang, X. *EMC Analysis Methods and Computational Models*; Beijing University of Posts and Telecommunication Press: Beijing, China, 2009. (In Chinese)
3. Zhou, Y.; Xie, Y.; Zhang, D.; Dong, N.; Chen, Y.; Jing, Y. Response of 10-kV Metal-Oxide Surge Arresters Excited by Nanosecond-Level Transient Electromagnetic Disturbances. *IEEE Trans. Electromagn. Compat.* **2021**, *63*, 614–621. [[CrossRef](#)]
4. Qin, F.; Chen, W.; Wang, X.; Huang, T.; Cui, Z.; Nie, X. Transient Response Characteristics of Metal Oxide Arrester under High-Altitude Electromagnetic Pulse. *Energies* **2022**, *15*, 3303. [[CrossRef](#)]
5. Chen, Y.; Xie, Y.; Zhang, D.; Zhou, Y.; Ren, D.; Gou, M.; Dong, N. 10-kV Transmission Line Experimental Platform for HEMP Immunity Test of Electrical Equipment in Operation. *IEEE Trans. Power Deliv.* **2021**, *36*, 1034–1040. [[CrossRef](#)]
6. Shu, Y.; Chen, W.; Li, Z. Experimental Research on Very-fast Transient Overvoltage in 1100-kV Gas-insulated Switchgear. *IEEE Trans. Power Deliv.* **2013**, *28*, 458–466. [[CrossRef](#)]
7. IEC 61000-2-10; Electromagnetic Compatibility (EMC)—Part 2-10: Environment—Description of HEMP Environment—Conducted Distribution. IEC: Geneva, Switzerland, 1998.
8. Zhou, B.; Shi, L.; Wang, J.; Chen, H.; Chen, B. *Electromagnetic Pulse and Its Engineering Protection*; National Defense Industry Press: Beijing, China, 2019. (In Chinese)
9. Anile, A.M.; Spinella, S.; Rinaudo, S. Stochastic Response surface Method and Tolerance Analysis in Microelectronics. *COMPEL Int. J. Comput. Math. Electr. Electron. Eng.* **2003**, *22*, 314–327. [[CrossRef](#)]
10. Ianoz, M.; Nicoara, B.; Radasky, W. Modeling of an EMP Conducted Environment. *IEEE Trans. Electromagn. Compat.* **1996**, *38*, 400–413. [[CrossRef](#)]
11. Stievano, I.S.; Manfredi, P.; Canavero, F.G. Stochastic Analysis of Multiconductor Cables and Interconnects. *IEEE Trans. Electromagn. Compat.* **2011**, *53*, 501–507. [[CrossRef](#)]
12. Manfredi, P.; Canavero, F.G. Polynomial Chaos for Random Field Coupling to Transmission Lines. *IEEE Trans. Electromagn. Compat.* **2012**, *54*, 677–680. [[CrossRef](#)]
13. Xiu, D.; Karniadakis, G.E. The Winner-Askey Polynomial Chaos for Stochastic Differential Equations. *SIAM J. Sci. Comput.* **2002**, *24*, 619–622. [[CrossRef](#)]
14. Xiu, D.; Karniadakis, G.E. Modeling Uncertainty in Steady State Diffusion Problems via Generalized Polynomial Chaos. *Comput. Methods Appl. Mech. Eng.* **2002**, *191*, 4927–4948. [[CrossRef](#)]
15. Ghanem, R.; Spanoes, P. Ingredients for a General Purpose Stochastic Finite Elements Implementation. *Comput. Methods Appl. Mech. Eng.* **1999**, *168*, 19–34. [[CrossRef](#)]
16. Finette, S. A Stochastic Representation of Environmental Uncertainty and Its Coupling to Acoustic Wave Propagation in Ocean Waveguides. *J. Acoust. Soc. Am.* **2006**, *120*, 2567–2579. [[CrossRef](#)]
17. Wang, T.; Gao, Y.; Gao, L. Statistical Analysis of Crosstalk for Automotive Wiring Harness via the Polynomial Chaos Method. *J. Balk. Tribol. Assoc.* **2016**, *22*, 512–526.
18. Spina, D.; Dhaene, T.; Knockaert, L.; Antonini, G. Polynomial Chaos-Based Macromodeling of General Linear Multiport Systems for Time-Domain Analysis. *IEEE Trans. Microw. Theory Tech.* **2017**, *65*, 1422–1433. [[CrossRef](#)]
19. Kheifets, I. Multivariate Specification Tests Based on a Dynamic Rosenblatt Transform. In *Computational Statistics and Data Analysis*; Elsevier: Amsterdam, The Netherlands, 2018; Volume 124, pp. 1–14.
20. Rosenblatt, M. Remarks on multivariate transformation. *Ann. Math. Stat.* **1952**, *23*, 470–472. [[CrossRef](#)]
21. Nicolas, M.; Bertrand, D.; Markus, N.; Carlos, R.; Farhad, R. Revisiting the Calculation of the Early Time HEMP Conducted Environment. *IEEE Trans. Electromagn. Compat.* **2021**, *63*, 111–124.
22. IEC 61000-2-9; Electromagnetic Compatibility (EMC)—Part 2-9: Environment—Description of HEMP Environment—Radiated Disturbance. IEC: Geneva, Switzerland, 1996.

Disclaimer/Publisher's Note: The statements, opinions and data contained in all publications are solely those of the individual author(s) and contributor(s) and not of MDPI and/or the editor(s). MDPI and/or the editor(s) disclaim responsibility for any injury to people or property resulting from any ideas, methods, instructions or products referred to in the content.